Commun Nonlinear Sci Numer Simulat 43 (2017) 261–270

Contents lists available at ScienceDirect

Commun Nonlinear Sci Numer Simulat

journal homepage: www.elsevier.com/locate/cnsns

Research paper

Frequency response reduced order model of primary resonance of electrostatically actuated MEMS circular plate resonators

Dumitru I. Caruntu*, Reynaldo Oyervides

University of Texas Rio Grande Valley, Mechanical Engineering Department, Edinburg, TX 78539, U.S.A.

ARTICLE INFO

Article history:
Received 28 February 2015
Revised 17 June 2016
Accepted 20 June 2016
Available online 1 July 2016

Keywords:
Primary resonance
MEMS circular plate resonators
Reduced order model
Soft AC electrostatic actuation

ABSTRACT

This paper deals with the amplitude-frequency response of soft AC electrostatically actuated MEMS clamped circular plates. Alternating Current (AC) frequency is near half natural frequency of the plate. This results in primary resonance of the system. Two methods are used and compared, namely the Method of Multiple Scales (MMS), and Reduced Order Model (ROM). Both methods are in excellent agreement for amplitudes less than 0.4 of the gap. For amplitudes between 0.4 and 1 of the gap only seven terms ROM accurately predicts the behavior of the system. The effects of the voltage and damping parameters on the frequency response are reported.

1. Introduction

Micro/Nano-Electromechanical Systems (M/NEMS) are excellent candidates for a large number of applications due to their low energy consumption and cost. Such applications are relay switches, frequency filters, mass flow sensors, accelerometers and resonators [1]. MEMS beams and/or plates consist of elastic beams [1] (cantilever or bridge) and/or elastic plates above a parallel rigid ground plate. MEMS plate structures are used as micropumps, microphones, and other micro sensors [2]. Micropumps cover a wide variety of applications such as drug delivery, chemical synthesis, chemical detection, cooling of electrical circuits, and inkjet printing [3]. Methods of actuation include piezoelectric, electrostatic, thermo-pneumatic, pneumatic, shape memory alloy, bimetallic and electromagnetic [3].

Electrostatic actuation of MEMS devices allows for simple design, effective fast response, and accurate control of the device. Both Alternating Current (AC) and/or Direct Current (DC) are used for electrostatic actuation. The voltage is applied between a suspended flexible microplate and a parallel fixed ground plate electrode. The voltage creates an electrostatic force between the plates causing the flexible microplate to deflect towards the ground plate. The deformation creates an elastic restoring force within the plate [4]. Electrostatically actuated MEMS plates experience an instability phenomenon, similar to buckling, called 'pull-in,' i.e. the microplate collapses onto and sticks to the ground plate. The critical voltage which causes the pull-in instability phenomenon is referred to as 'pull-in voltage' [2,4]. The pull-in instability limits the MEMS device's maximum displacement. This is a major concern for the design and testing of MEMS devices [5]. The pull-in phenomena occur due to the nonlinearity of the electrostatic force which is inversely proportional to the square of the distance of the gap between the flexible plate and the ground plate [2]. Saddle-node bifurcation is a type of instability [5] experienced

* Corresponding author. Fax: +1 956 665 3527.
E-mail address: dumitru.caruntu@utrgv.edu, caruntud2@asme.org, dcaruntu@yahoo.com (D.I. Caruntu).

http://dx.doi.org/10.1016/j.cnsns.2016.06.032
1007-5704/

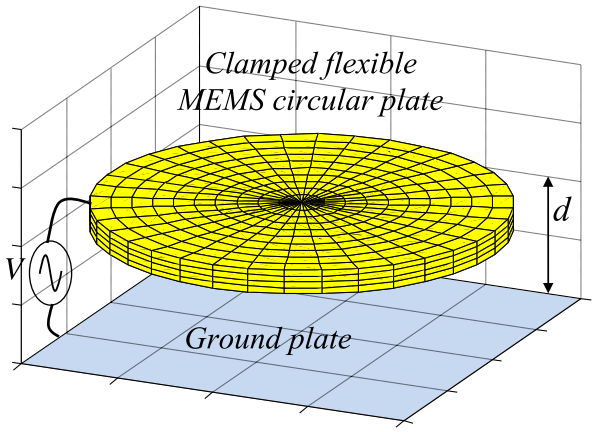

Fig. 1. Electrostatically actuated MEMS uniform circular plate suspended above a parallel ground plate.

by nonlinear systems. The stability of these devices is highly sensitive to physical parameters such as its initial amplitude, initial velocity, frequency of excitation and the environment they are exposed to [6]. Slight changes in temperature cause the resonance frequency of the device to change [7]. The influence of temperature on the behavior of devices such as annular and circular plates has been investigated in an effort to improve their stability [8,9]. MEMS are highly sensitive. Energy dissipation becomes more significant as their sizes keep decreasing [7]. One cause of energy dissipation is thermoelastic damping, which was found to be a significant cause of energy loss near room temperatures for MEMS resonators [7].

Reduced Order Model (ROM) is a numerical method that can be used for investigating the behavior of MEMS. Nayfeh and Vogl have studied the behavior of electrically actuated clamped circular plates using ROM method [10,11]. Another method that can be used is the method of multiple scales (MMS) which is an analytical perturbation method. Caruntu et al. [6,12] investigated the primary resonance of microcantilevers using MMS and ROM. Their model takes into consideration the effects of Casimir force and the fringe effect. Similar numerical and analytical approaches have been conducted for investigating the behavior of clamped-clamped arches. A softening effect before pull-in has been reported in this case [13]. Amplitude frequency response is a very important characteristic of MEMS resonators and it consists of steady-state amplitudes of vibration dependence on the excitation frequency while the voltage is kept constant [12,14,15]. Bifurcation points of the frequency response provide the frequencies at which the stability of the system changes. Therefore, amplitude frequency responses are used to predict the changes in stability, pull-in, and hardening or softening effects. Other investigations using MMS and ROM to obtain the amplitude frequency response of a resonator have been published by Caruntu and Martinez [14], Caruntu et al. [12], Caruntu and Knecht [6], and Caruntu and Taylor [16].

This paper investigates the amplitude-frequency response of axisymmetric vibrations of clamped circular plates electrostatically actuated by soft AC voltage of frequency near half natural frequency of the plate. This results in primary resonance of the system as showed afterwards. This investigation is conducted using MMS and two integration techniques for the ROM method, one uses AUTO to obtain the amplitude-frequency response, and the second uses Matlab to obtain time responses to additionally test the behavior of the system.

To the best of our knowledge, this is the first time when a direct comparison between MMS and ROM up to seven terms (seven modes of vibration) for the primary resonance frequency response of electrostatically actuated MEMS circular plates is conducted. It is showed that MMS is valid for amplitudes less than 0.4 of the gap, beyond this point being unreliable. Conversely, ROM is valid for all range of amplitudes provided a sufficient number of terms are considered. In this work the convergence of ROM shows that seven terms provide an accurate behavior of the primary resonance of the MEMS plate. The effects of voltage and damping parameters on the frequency response show opposite effects. The increase in voltage and increase in damping result in increase and decrease of the nonlinear effect in the system, respectively.

2. Differential equation of motion

The system consists of a deformable clamped circular plate suspended above a parallel rigid ground plate as shown in Fig. 1. R is the outer radius of the uniform circular plate, h the thickness, d the gap between the plates, and w the deflection of the plate. The dimensionless equation of axisymmetric vibrations of circular plates under electrostatic actuation given by AC voltage only is as follows [17]

$$\frac{\partial^2 u}{\partial t^2}+\mu\frac{\partial u}{\partial t}+\frac{\partial^4 u}{\partial r^4}+\frac{2}{r}\frac{\partial^3 u}{\partial r^3}-\frac{1}{r^2}\frac{\partial^2 u}{\partial r^2}+\frac{1}{r^3}\frac{\partial u}{\partial r}=\frac{\delta\cos^2\Omega^* t}{(1-u)^2} \tag{1}$$

where t is dimensionless time, r dimensionless radial coordinate, and $u(r, t)$ dimensionless deflection of the plate. They are given by

$$u = \frac{\hat{u}}{d}, \quad r = \frac{\hat{r}}{R}, \quad t = \hat{t}\sqrt{\frac{D}{\rho h R^4}} \tag{2}$$

The variables $\hat{u}$, $\hat{r}$, $\hat{t}$ are the corresponding dimensional variables. The parameters from Eq. (1) are μ dimensionless damping coefficient, δ dimensionless voltage coefficient, Ω^* dimensionless AC excitation frequency, where D is flexural rigidity. They are given by

$$\mu = 2c_1\sqrt{\frac{R^4}{\rho h D}}, \quad \delta = \frac{R^4\varepsilon^* V_0^2}{2Dd^3}, \quad \Omega^* = \Omega\sqrt{\frac{\rho h R^4}{D}}, \quad D = \frac{Eh^3}{12(1-\nu^2)} \tag{3}$$

Dimensional characteristics of a typical MEMS circular plate used in this work can be found in Refs. [17,18]. Two methods are used in his work for investigating the frequency response of the primary resonance of the electrostatically actuated microplate, namely MMS and ROM method.

3. Method of multiple scales

MMS is a perturbation method valid for weakly nonlinear systems and small amplitudes and it is the first method of investigation used in this work. In this work soft actuation and weak damping are considered. Two scales are considered for this MMS model, namely the fast scale $T_0 = t$ and the slow scale $T_1 = \varepsilon \cdot t$. In order to use MMS, the electrostatic terms of the equation are expanded in Taylor series. Therefore Eq. (1) becomes

$$\frac{\partial^2 u}{\partial t^2} + \varepsilon\mu\frac{\partial u}{\partial t} + P[u] = \varepsilon\delta(1 + 2u + 3u^2 + 4u^3)\cos^2\Omega^* t \tag{4}$$

where the operator P is given by

$$P = \left[\frac{\partial^4}{\partial r^4} + \frac{2}{r}\frac{\partial^3}{\partial r^3} - \frac{1}{r^2}\frac{\partial^2}{\partial r^2} + \frac{1}{r^3}\frac{\partial}{\partial r}\right] \tag{5}$$

The bookkeeping device ε is used on the assumed weakly nonlinear terms and damping. Consider a first order MMS expansion of the deflection as follows

$$u = u_0 + \varepsilon \cdot u_1 \tag{6}$$

where u_0 and u_1 are the zero order and first order components of the solution to be determined. The derivative with respect to time, using the time scales T_0 and T_1, is $\partial/\partial t = D_0 + \varepsilon D_1, D_0 = \partial/\partial T_0, D_1 = \partial/\partial T_1$. The AC voltage in this work is of frequency Ω^* near half the natural frequency ω_k of the plate. The AC frequency Ω^* can be written as

$$\Omega^* = \frac{\omega_k}{2} + \varepsilon\sigma \tag{7}$$

where σ is the frequency detuning parameter. Due to the fact that the electrostatic force is proportional to the square of the voltage the system experiences primary resonance. Substituting Eqs. (6,7) and the time derivative in terms of the two time scales into Eq. (4), expanding the resulting equation, and then collecting the ε^0 and ε^1 terms and setting their sums equal to zero, results into two problems, namely zero-order and first-order problems given by

$$\varepsilon^0 : D_0^2 u_0 + P[u_0] = 0 \tag{8}$$

$$\begin{aligned}\varepsilon^1 : D_0 u_1 + P[u_1] = {} & -2D_0 D_1 u_0 - \mu D_0 u_0 \\ & + \delta\cos^2\left(\frac{1}{2}\omega_k T_0 + \sigma T_1\right)\left[1 + 2u_0 + 3u_0^2 + 4u_0^3\right]\end{aligned} \tag{9}$$

The solution of Eq. (8) along with the boundary conditions for a clamped uniform circular plate give the solution for u_0

$$u_0 = \phi_k(r)[A(T_1)e^{i\omega_k T_0} + \bar{A}(T_1)e^{-i\omega_k T_0}] \tag{10}$$

where ϕ_k are the mode shapes of vibration and ω_k the corresponding natural frequencies, Table 1. The equation of the mode shapes of vibration for a circular plate is given by

Table 1
First seven dimensionless natural frequencies for clamped circular plates.

	$N=1$	$N=2$	$N=3$	$N=4$	$N=5$	$N=6$	$N=7$
ω_k	10.216	39.771	89.104	158.183	247.005	355.568	483.872

$$\phi_k(r) = \left(\frac{J_0(\sqrt{\omega_k}r)}{J_0(\sqrt{\omega_k})} - \frac{I_0(\sqrt{\omega_k}r)}{I_0(\sqrt{\omega_k})}\right) \tag{11}$$

For non-uniform structures, dynamic modal characteristics and methods of finding them can be found in Refs. [19–23]. Substituting Eq. (10) into Eq. (9), expanding the right hand side of the resulting equation, multiplying it by the operator given below

$$\int_0^1 \cdot\, r\phi_k(r)dr \tag{12}$$

and set it equal to zero in order to satisfy the solvability condition of orthogonality to any solution of the homogeneous equation, and then collecting the secular terms ($e^{i\omega_k T_0}$) and set them equal to zero gives the secular terms equation as follows

$$\begin{aligned}&-2A'i\omega_k g_2 - \mu\phi i\omega_k A g_2 + \frac{1}{4}\delta e^{2i\sigma T_1} g_1 + \delta A g_2\\ &\quad + A^2\left(\frac{3}{4}\delta e^{-2i\sigma T_1}\right)g_3 + 2A\bar{A}\left(\frac{3}{4}\delta e^{2i\sigma T_1}\right)g_3 + 6\delta A^2\bar{A}g_4 = 0\end{aligned} \tag{13}$$

where A' is the derivative of the complex amplitude A with respect to the slow time scale T_1, and g_k coefficients are given by

$$g_m = \int_0^1 r\phi_k^m(r)dr, \quad m = 1, 4 \tag{14}$$

The complex amplitude A given by

$$A = \frac{1}{2}ae^{i\theta} \quad \text{and} \quad \bar{A} = \frac{1}{2}ae^{-i\theta} \tag{15}$$

where a and θ are real amplitude and phase of the motion. Replacing Eq. (15) into Eq. (13), and separating the imaginary and real terms, results into two equations. Denoting

$$\gamma = 2\sigma T_1 - \theta \tag{16}$$

the steady-state solutions ($a' = \gamma' = 0$) are given by

$$a = \frac{4}{3}\frac{\mu\omega_k g_2}{\delta g_3 \sin\gamma} \pm \sqrt{\frac{16}{9}\frac{\mu^2\omega_k^2 g_2^2}{\delta^2 g_3^2 \sin^2\gamma} - \frac{4}{3}\frac{g_1}{g_3}} \tag{17}$$

$$\sigma = \left(-\frac{1}{8}\frac{g_1}{a} - \frac{9}{32}ag_3\right)\frac{\delta\cos\gamma}{\omega_k g_2} - \frac{1}{4}\frac{\delta}{\omega_k} - \frac{3\delta a^2 g_4}{8\omega_k g_2} \tag{18}$$

4. Reduced order model

Reduced Order Model (ROM) is the second method used in this research. ROM is a numerical method valid for both weak and strong nonlinearities and both low and high amplitudes of vibrations provided a sufficient number of terms (modes of vibration) is considered. ROM is more accurate than MMS, it gives a better understanding of pull-in instability of the system. A comparison between the two methods is conducted afterwards. The dimensionless deflection $u(r,t)$, i.e. the solution of Eq. (1), is considered as

$$u(r,t) = \sum_{i=1}^{N} u_i(t)\phi_i(r) \tag{19}$$

where N is the number of ROM terms, $\phi_i(r)$ mode shapes given by Eq. (11), and $u_i(t)$ time functions to be determined. Eq. (1) is multiplied by $(1-u)^2$ to result into an equation with no denominators. Substituting Eq. (19) into the resulting equation and multiplying it by the operator given by Eq. (12) for $k = n$, one finds the N ROM equations as follows:

$$\begin{aligned}&\sum_{i=1}^{N}\frac{\partial^2 u_i}{\partial t^2}\left(\int_0^1 r\phi_n\phi_i dz - 2\sum_{j=1}^{N}u_j\int_0^1 r\phi_n\phi_i\phi_j dz + \sum_{jk}^{N}u_j u_k\int_0^1 r\phi_n\phi_i\phi_j\phi_k dz\right)\\ &= -\mu\left(\sum_{i=1}^{N}\frac{\partial u_i}{\partial t}\int_0^1 r\phi_n\phi_i dz - 2\sum_{ij}^{N}\frac{\partial u_i}{\partial t}u_j\int_0^1 r\phi_n\phi_i\phi_j dz + \sum_{ijk}^{N}\frac{\partial u_i}{\partial t}u_j u_k\int_0^1 r\phi_n\phi_i\phi_j\phi_k dz\right)\\ &\quad - \sum_{i=1}^{N}\omega_i^2 u_i\int_0^1 r\phi_n\phi_i dz + 2\sum_{ij}^{N}\omega_i^2 u_i u_j\int_0^1 r\phi_n\phi_i\phi_j dz - \sum_{ijk}^{N}\omega_i^2 u_i u_j u_k\int_0^1 r\phi_n\phi_i\phi_j\phi_k dz\\ &\quad + \delta\int_0^1 r\phi_n dxz\cos^2(\Omega t)\end{aligned} \tag{20}$$

Table 2
System constants.

Permitivity of free space	ε^*	8.854e-12	$C^2/N/m^2$	[17,18]
Young's modulus	E	150.6	GPa	[17,18]
Poisson's ratio	ν	0.23		[17,24]
Density of material	ρ	2330.0	kg/m^3	[17,18]

Table 3
Dimensional system parameters.

Radius of plate	R	250.0	μm	[17,18]
Initial gap distance	d	1.014	μm	[17,18]
Plate thickness	h	3.01	μm	[17,18]
Damping	c_1	2.014	Ns/m^3	[17]
Voltage	V_0	1.044	V	[17]

Table 4
Dimensionless system parameters.

Voltage parameter	δ	0.200
Damping parameter	μ	0.005

where $n = 1,2,\ldots,N$. The system of N second order differential Eq. (20) is transformed in a system of $2N$ first order differential equations which is then integrated using two software packages: Matlab for finding time responses of the system, and AUTO 07P, a software for continuation and bifurcation problems, for finding the frequency response of the system. The time responses given by Matlab are used to obtain the steady-state amplitudes in order to additionally test the results given by ROM using AUTO. ROM simulations using AUTO are conducted for $N = 2,3,4,5,6,7$ terms in order to investigate the convergence of the method. The frequency response is the relationship between the amplitude of vibration and the frequency of electrostatic excitation, as shown in the next section. Different cases are shown to study the effects of the actuating voltage, and the damping on the frequency response. ROM numerical simulations are conducted for Ω^* near half natural frequency of the plate, Eq. (8) for $\varepsilon = 1$, leading the system to primary resonance. ROM results are then compared to MMS results.

5. Frequency response of primary resonance – numerical simulations

Numerical simulations are conducted for investigating the frequency response of the primary resonance of the electrostatically actuated MEMS circular plate. The mode shapes of the clamped circular plate are given by Eq. (11). The corresponding first seven natural frequencies are given in Table 1. The constants of the system and the dimensions of a typical MEMS circular plate are given in Tables 2 and 3, respectively. The dimensionless parameters μ, δ are found using Eq. (3) and Tables 2 and 3, and they are given in Table 4. In this paper soft electrostatic AC actuation is used. The AC frequency is near half fundamental natural frequency of the circular plate, i.e ω_1 in Table 1 and $k = 1$ in Eqs. (7), (17) and (18), which results in a primary resonance phenomenon [17].

Fig. 2 shows the amplitude-frequency response of the electrostatically actuated MEMS circular plate in the case of soft AC of frequency near half fundamental natural frequency of the plate using two methods, namely MMS and ROM. In the ROM method seven terms (seven modes of vibration) are used. In the horizontal axis is the detuning frequency parameter, see Eq. (7) for $\varepsilon = 1$, and in the vertical axis is U_{max} the steady-state amplitude of the center of the MEMS plate. The amplitude-frequency behavior of the MEMS plate is discussed next using ROM results. There are three branches of the response. The solid branches are stable branches. The dash branches are unstable. There are two situations to be discussed, first when the system reached steady-state and the frequency is swept up and down, and second when the frequency and initial amplitude (other than steady-state) are given and the frequency is kept constant. In the first situation, as the frequency is swept up the steady-state amplitude increases along branch 1 until reaches point A of amplitude 0.51 of the gap. At this point the plate loses stability and the amplitude suddenly jumps to a value of 1 (the amplitude reaches the value of the gap), i.e. a pull-in phenomenon occurs (contact between the MEMS plate and the ground plate). A is a saddle-node bifurcation point. The arrows to the right and up show this behavior. As the frequency is swept down from larger frequencies the amplitude increases along branch 3 until reaches point C where the system loses stability and undergoes a pull-in phenomenon. The arrows to the left and up show this behavior. In the second situation, when the frequency is kept constant, the behavior of the system depends on its AC frequency and its initial amplitude. If the frequency is less than the frequency of point B then regardless of initial amplitude the plate settles to an amplitude on branch 1. If the frequency is between the frequencies of points A and B, then the behavior of the system depends on the initial amplitude. Branch 2 is unstable. Therefore for any initial amplitude below branch 2, the plate settles to a steady-state amplitude on branch 1. Fig 3a and 3b show time response examples in this case. If the initial amplitude is above branch 2, then the system undergoes a pull-in phenomenon. Fig. 3c shows a time response example in this case. If the frequency is between the frequencies of points A and C, this is

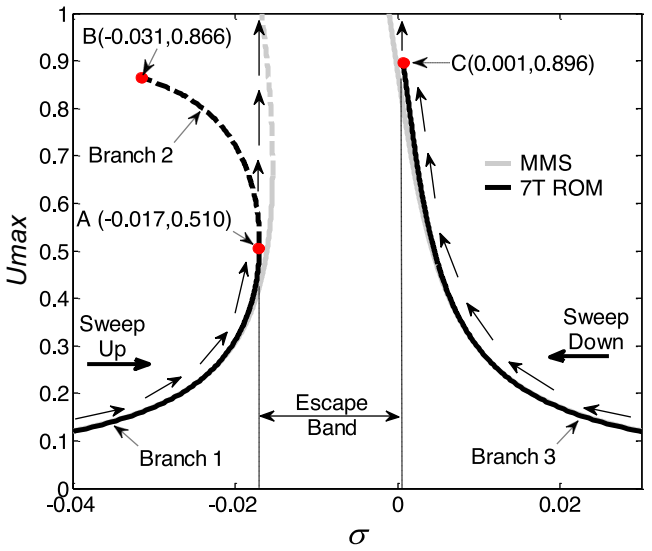

Fig. 2. Amplitude frequency response of primary resonance (AC frequency near half fundamental natural frequency) for MEMS clamped uniform circular plate using MMS and seven terms ROM (7T ROM). $\mu = 0.005$, $\delta = 0.2$.

called escape band, Fig. 2, then regardless of the value of initial amplitude, the plate undergoes a pull-in phenomenon. Fig. 3d shows an example of time response in this case. If the frequency is greater than the frequency of point *C* regardless the value (less than the gap) of the initial amplitude, the plate settles to a steady-state amplitude on branch 3. Fig. 3e and 3f show the time responses around point *B*. Initial amplitude of 0.9 of the gap and $\sigma = -0.029$ places the initial point above and to the right hand side of point *B*. Figs. 2 and 3e are in agreement both showing a pull-in phenomenon. Initial amplitude of 0.9 of the gap and $\sigma = -0.035$ places the initial point above and to the left hand side of point *B*. Figs. 2 and 3f are in agreement both showing the system settles to an amplitude less than 0.2 of the gap on branch 1.

MMS and ROM are in excellent agreement for amplitudes less than 0.4 of the gap. For larger amplitudes ROM predicts the behavior of the MEMS plate, while MMS fails. This is expected since MMS is a method valid for weak nonlinearities and small amplitudes. MMS 1) overestimates both the amplitude and frequency of the bifurcation point *A*, point extremely important for sensing applications. 2) It does not predict the pull-in instability point *C*. 3) It underestimates the range of frequencies and the amplitudes of the unstable branch 3.

In conclusion only seven terms ROM (7T ROM) accurately predicts the behavior of the MEMS plate for all amplitudes.

6. Discussion and conclusions

Fig. 4 illustrates the convergence of the ROM method. The number of terms considered in the method is between two and seven. One can notice that the bifurcation point *A* is predicted by any number of terms in the ROM. Conversely, only the seven terms ROM predicts the pull-in instability point *C* and the upper limit of the unstable branch point *B*. Fig. 5 shows a detail around point *B* of the convergence. In what follows the seven terms ROM is used to investigate the effects of the voltage and damping parameters.

Fig. 6 shows the effect of the voltage parameter on the frequency response. One can notice that if the voltage parameter is small the system has a linear behavior. As the voltage parameter increases the system experiences a nonlinear behavior. The frequency of the bifurcation point *A* is shifted to lower frequencies while its amplitude is not significantly affected. If the voltage is large enough then an instability pull-in point *C* is born. Also, the escape band enlarges.

Fig. 7 illustrates the effect of the damping parameter on the response. Small damping results into a nonlinear behavior of the system. As the damping increases the bifurcation point *A* is shifted to higher frequencies and amplitudes, the instability point *C* to lower frequencies, and overall the range of the escape band reduces. If the damping is large enough, then the branches collapse onto each other resulting only one branch and a linear behavior of the system, with no pull-in phenomenon possible.

One should mention that the approach in this work, namely using MMS and ROM methods, have been successfully used not only for voltage response [17] of MEMS plates, but also for frequency and voltage responses of electrostatically actuated Single Wall Carbon Natotubes (SWCNT), Ref. [25,26], and electrostatically actuated MEMS beam resonators [6,11–17]. "A remark is necessary. Since model order reduction is a technique to reduce complex models to an associated state-space dimension, i.e. a number of degrees of freedom, MMS in this work can be considered a reduced-order model, namely one term (one mode of vibration) reduced order model as it uses only one mode of vibration. MMS is an analytical-approximate method solving one term reduced order model, while ROM with more than two terms are numerically integrated," [25]. In

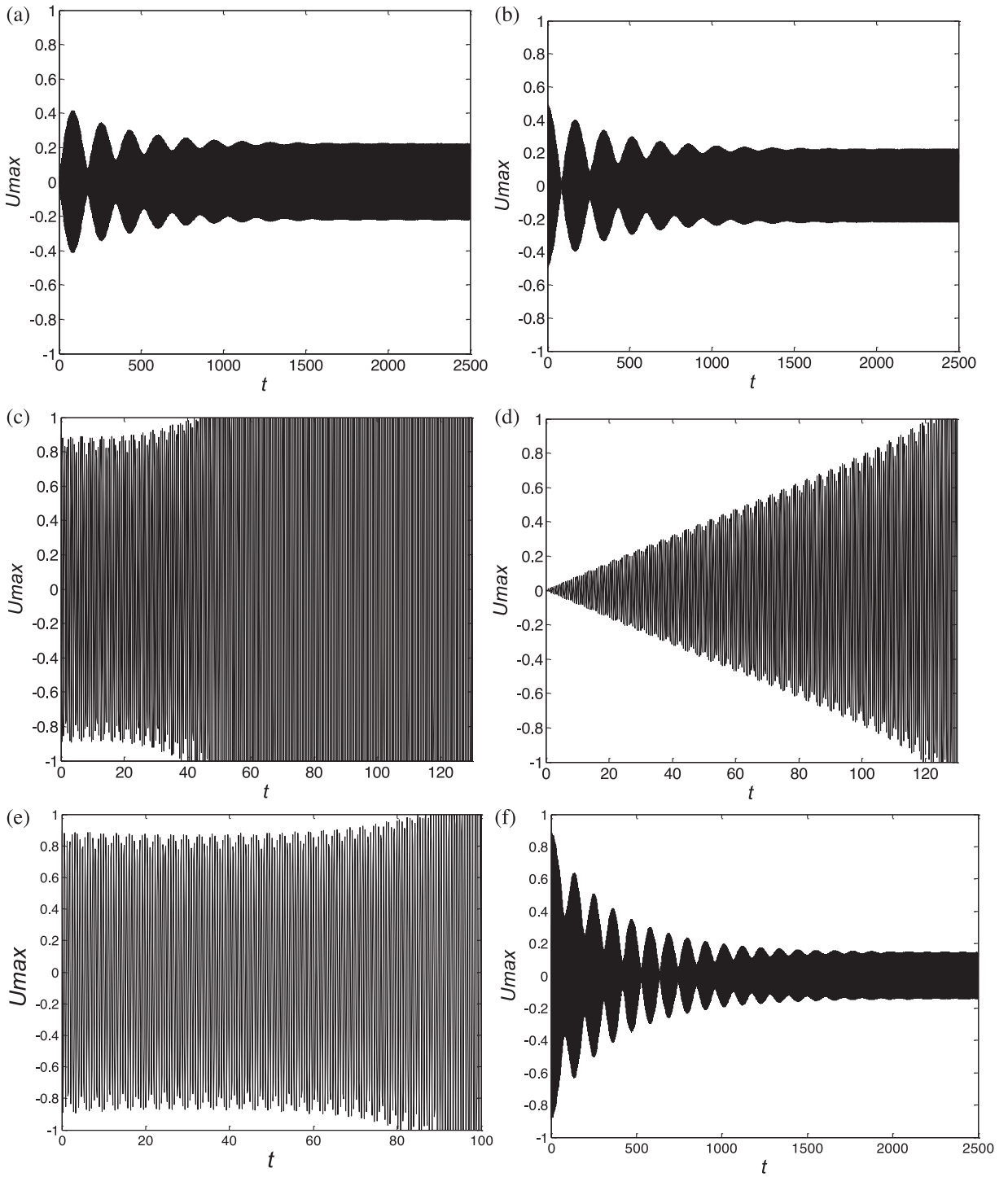

Fig. 3. (a) Time response using 7T ROM for MEMS clamped circular plate for. AC frequency near half fundamental natural frequency. Initial amplitude $U_0 = 0$; $\delta = 0.2$, $\mu = 0.005$, $\sigma = -0.025$. (b) Time response using 7T ROM for MEMS clamped circular plate for. AC frequency near half fundamental natural frequency. Initial amplitude $U_0 = 0.5$; $\delta = 0.2$, $\mu = 0.005$, $\sigma = -0.025$. (c) Time response using 7T ROM for MEMS clamped circular plate for. AC frequency near half fundamental natural frequency. Initial amplitude $U_0 = 0.9$; $\delta = 0.2$, $\mu = 0.005$, $\sigma = -0.025$**.** (d) Time response using 7T ROM for MEMS clamped circular plate for. AC frequency near half fundamental natural frequency. Initial amplitude $U_0 = 0$; $\delta = 0.2$, $\mu = 0.005$, $\sigma = -0.01$. (e) Time response using 7T ROM for MEMS clamped circular plate for. AC frequency near half fundamental natural frequency. Initial amplitude $U_0 = 0.9$; $\delta = 0.2$, $\mu = 0.005$, $\sigma = -0.029$. (f) Time response using 7T ROM for MEMS clamped circular plate for. AC frequency near half fundamental natural frequency. Initial amplitude $U_0 = 0.9$; $\delta = 0.2$, $\mu = 0.005$, $\sigma = -0.035$.

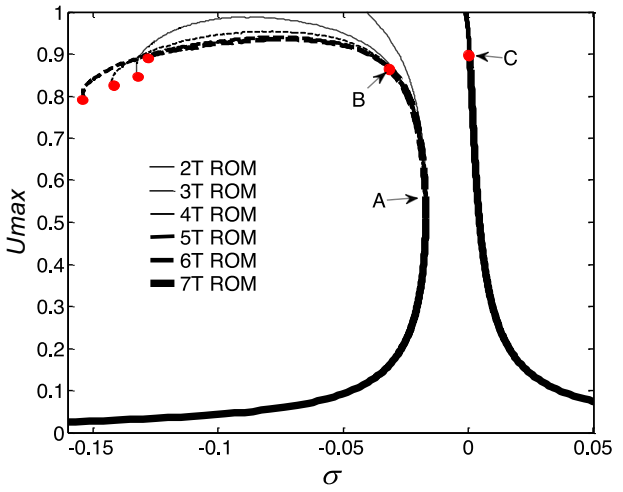

Fig. 4. ROM convergence of amplitude frequency response for MEMS clamped circular plate using two terms (2T ROM), three terms (3T ROM), ..., seven terms (7T ROM). AC frequency near half fundamental natural frequency. $\mu = 0.005$, $\delta = 0.2$.

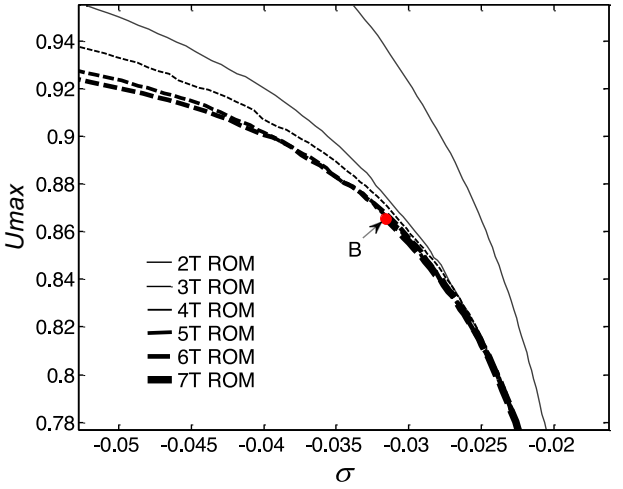

Fig. 5. ROM convergence detail from Fig. 4. AC frequency near half fundamental natural frequency. $\mu = 0.005$, $\delta = 0.2$.

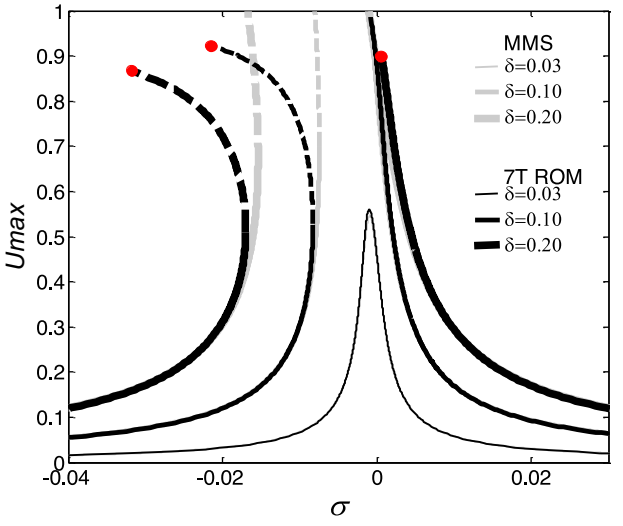

Fig. 6. Effect of voltage parameter δ on the amplitude frequency response for MEMS clamped circular plate using seven terms ROM (7T ROM). AC frequency near half fundamental natural frequency. $\mu = 0.005$.

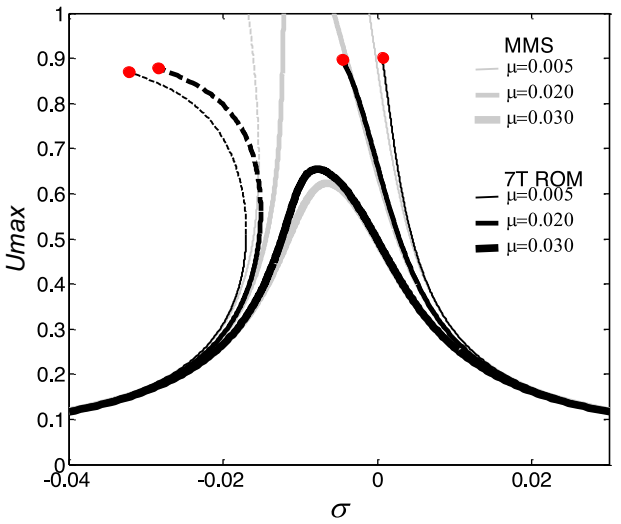

Fig. 7. Effect of damping parameter μ on the amplitude frequency response for MEMS clamped circular plate using seven terms ROM (7T ROM). AC frequency near half fundamental natural frequency. $\delta = 0.2$.

conclusion, Figs. 2, 4 and 5 do not show a non-convergence of the ROM. Moreover these figures show ROM convergence from one term ROM solved using MMS, Fig. 2, and from two terms to seven terms ROM solved numerically, Figs. 4 and 5, using AUTO 07P, Ref. [27], a continuation and bifurcation software for ordinary differential equations. The convergence of the ROM with the number of modes, compared against experimental data, has been reported in the literature [28].

One of the limitations of this paper is that it does not include experimental work. This will be the focus of a future investigation.

Acknowledgements

This material is based on research sponsored by Air Force Research Laboratory under agreement number FA8650-07-2-5061. The U.S. Government is authorized to reproduce and distribute reprints for Governmental purposes notwithstanding any copyright notation thereon. The views and conclusions contained herein are those of the authors and should not be interpreted as necessarily representing the official policies or endorsements, either expressed or implied, of Air Force Research Laboratory or the U.S. Government.

REFERENCES

[1] Mojahedi M, Moghimi Zand M, Ahmadian MT. Static pull-in analysis of electrostatically actuated microbeams using homotopy perturbation method. Appl Math Model 2010;34:1032–41.
[2] Talebian S, Rezazadeh G, Fathalilou M, Toosi B. Effect of temperature on pull-in voltage and natural frequency of an electrostatically actuated microplate. Mechatronics 2010;20:666–73.
[3] Yih T, Wei C, Hammad B. Modeling and characterization of a nanoliter drug-delivery MEMS micropump with circular bossed membrane. Nanomedicie 2005;1:164–75.
[4] Moghimi Zand M, Ahmadian MT. Application of homotopy analysis method in studying dynamic pull-in instability of Microsystems. Mech Res Commun 2009;36:851–8.
[5] Zhang Y, Zhao Y. Numerical and analytical study on the pull-in instability of micro-structure under electrostatic loading. Sensors Actuat A 2006;127:366–80.
[6] Caruntu DI, Knecht MW. On nonlinear response near-half natural frequency of electrostatically actuated microresonators. Int J Struct Stab Dyn 2011;11:641–72.
[7] Sun Y, Tohmyoh H. Thermoelastic damping of the axisymmetric vibration of circular plate resonators. J Sound Vib 2009;319:392–405.
[8] Arafat H, Nayfeh A, Faris W. Natural frequencies of heated annular and circular plates. Int J Solids Struct 2004;41:3031–51.
[9] Faris W, Nayfeh AH. Mechanical response of a capacitive microsensor under thermal load. Communications in Nonlinear Science and Numerical Simulation 2007;12:776–83.
[10] Nayfeh A, Vogl G. A reduced-order model for electrically actuated clamped circular plates. J Micromech Microeng 2005;15:684–90.
[11] Nayfeh A, Younis M, Abdel-Rahman E. A reduced-order model for electrically actuated microbeam-based MEMS. J Microelectromech Syst 2003;12(5):672–80.
[12] Caruntu DI, Martinez I, Taylor KN. Reduced order model analysis of frequency response of alternating current near half natural frequency electrostatically actuated MEMS cantilevers. J Comput Nonlinear Dyn 2013;8 031011-1–031011-6.
[13] Ouakad H, Younis M. The dynamic behavior of MEMS arch resonators actuated electrically. Int J Non Linear Mech 2010;45:704–13.
[14] Caruntu DI, Martinez I. Reduced order model of parametric resonance of electrostatically actuated MEMS cantilever resonators. Int J Non Linear Mech 2014;66:28–32.
[15] Ghayesh M, Farokhi H, Amabili M. Nonlinear behavior of electrically actuated MEMS resonators. Int J Eng Sci 2013;71:137–55.
[16] Caruntu DI, Taylor KN. Bifurcation type change of AC electrostatically actuated MEMS resonators due to DC bias. Shock Vib 2014;2014:9 Article ID 542023.
[17] Caruntu DI, Oyervides R. Voltage response of primary resonance of electrostatically actuated MEMS clamped circular plates resonatos. J Comput Nonlinear Dyn 2014;11:041021-1–041021-7.

[18] Liao LD, Chao PCP, Huang CW, Chiu CW. DC dynamic and static pull-in predictions and analysis for electrostatically actuated clamped circular micro–plates based on a continuous model. J Micromech Microeng 2010;20:025013.
[19] Caruntu DI. Dynamic modal characteristics of transverse vibrations of cantilevers of parabolic thickness. Mech Res Commun 2009;33(3):391–404.
[20] Caruntu DI. Classical Jacobi polynomials, closed-form solutions for transverse vibrations. J Sound Vib 2007;306(3-5):467–94.
[21] Caruntu DI. Self-adjoint differential equations for classical orthogonal polynomials. J Comput Appl Math 2005;180(1):107–18.
[22] Caruntu DI. Factorization of self-adjoint ordinary differential equations. J Appl Math Comput 2013;219:7622–31.
[23] Caruntu DI. Eigenvalue singular problem of factorized fourth-order self-adjoint differential equations. J Appl Math Comput 2013;224:603–10.
[24] Bank-Sills L, Hikri Y, Krylov S, Fourman V, Gerson Y, Bruck HA. Measurement of Poisson's ratio by means of a direct tension test on micron-sized specimens. Sensors and Actuators A 2011;169(1):98–114.
[25] Caruntu DI, Luo L. Frequency response of primary resonance of electrostatically actuated CNT cantilevers. Nonlinear Dyn 2014;78:1827–37.
[26] Caruntu DI, Luo L. Bifurcation and pull-in voltages of primary resonance of electrostatically actuated SWCNT cantilevers to include van der Waals effect. Meccanica; 2016. doi:10.1007/s11012-016-0461-8.
[27] Doedel EJ, Oldeman BE. AUTO-07P: continuation and bifurcation software for ordinary differential equations. Montréal, Canada: Concordia University; 2009.
[28] Younis M. Analytical expressions for the electrostatically actuated curled beam problem. Microsyst Technol 2015;21:1709–17.